Accepted Manuscript

Design, synthesis and evaluation of novel tacrine-multialkoxybenzene hybrids as multi-targeted compounds against Alzheimer's disease

Chao Zhang, Qiao-Yi du, Lang-Di Chen, Wen-Hao Wu, Si-Yan Liao, Li-Hong Yu, Xin-Tong Liang

PII: S0223-5234(16)30260-4

DOI: 10.1016/j.ejmech.2016.03.077

Reference: EJMECH 8502

To appear in: *European Journal of Medicinal Chemistry*

Received Date: 30 December 2015

Revised Date: 24 March 2016

Accepted Date: 25 March 2016

Please cite this article as: C. Zhang, Q.-Y. du, L.-D. Chen, W.-H. Wu, S.-Y. Liao, L.-H. Yu, X.-T. Liang, Design, synthesis and evaluation of novel tacrine-multialkoxybenzene hybrids as multi-targeted compounds against Alzheimer's disease, *European Journal of Medicinal Chemistry* (2016), doi: 10.1016/j.ejmech.2016.03.077.

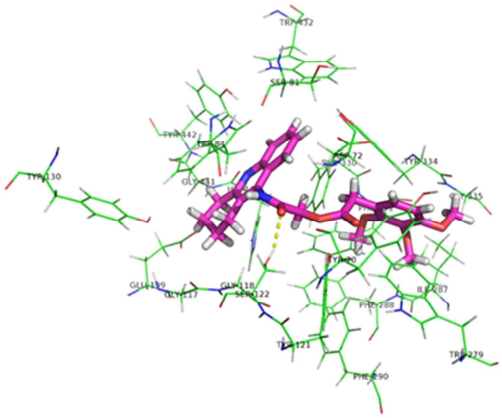

Molecular modeling with *Tc*AChE and **7c**

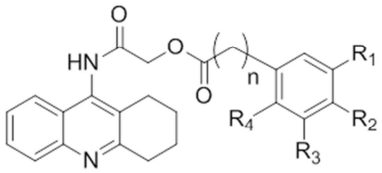

7c, R^2=R^3=R^4=OMe, R^1=H, n=1

IC_{50} (nM):

AChE	BChE	Aβ (1-42) aggregation
5.63	364	51.81

Design, synthesis and evaluation of novel tacrine-multialkoxybenzene hybrids as multi-targeted compounds against Alzheimer's disease

Chao Zhang [a, *], Qiao-Yi Du [a], Lang-Di Chen [a], Wen-Hao Wu [a], Si-Yan Liao [a], Li-Hong Yu [a] and Xin-Tong Liang [a]

[a, *] *School of Pharmaceutical Sciences, Guangzhou Medical University, Xinzao, Panyu District, Guangzhou, 511436, P. R. China*

Abstract: A series of benzoates (or phenylacetates or cinnamates) – tacrine hybrids (7**a**-**o**) were designed, synthesized and evaluated as multi-potent anti-Alzheimer drug candidates. The screening results showed that most of them exhibited a significant ability to inhibit ChEs, certain selectivity for AChE over BuChE and strong potency inhibitory of self-induced β-amyloid (Aβ) aggregation. All IC_{50} values of biological activity were at the nanomolar range. Especially, compound **7c** displayed the greatest ability to inhibit AChE with an IC_{50} value of 5.63 nM and the highest selectivity with ratio of BuChE/AChE value of 64.6. Moreover, it also exhibited a potent inhibitory of Aβ aggregation with an IC_{50} value of 51.81 nM. A Lineweaver-Burk plot and molecular modeling study showed that compound **7c** targeted both the CAS and PAS of ChEs. A structure-activity relationship analysis suggested that the electron density of aromatic ring which was linked with tacrine through acetyl group played a significant role in determining the inhibitory activity.

Keywords: Tacrine, Multi-target-directed ligands, Alzheimer's disease, Cholinesterase inhibitors, Self-induced Aβ aggregation.

1. Introduction

Alzheimer's disease (AD) is a progressive neurodegenerative brain disorder that is characterized by dementia, cognitive impairment, memory loss, severe behavioral abnormalities and ultimately death [1,2]. It is estimated that more than 18 million people presently suffer from AD, and the number of patients is expected to sharply increase to 114 million by 2050[3]. The vast number of people requiring constant care and related services will severely strain medical, monetary and human resources. Consequently, the developing treatments that slow or halt the disease progression have become imperative. Despite enormous efforts devoted to research in AD and many factors have been found to be implicated in AD over past decades, its etiology and pathogenesis remain unclear. To date AD is thought to be a complex, multifactorial syndrome with many related molecular lesions contributing to its pathogenesis[4-8]. Several factors including low levels of acetylcholine (ACh),

amyloid-β(Aβ) deposits, oxidative stress and dyshomeostasis of biometals have been considered to play definitive roles in its etiology, and several hypotheses based on these factors have been proposed to explain the mechanism of AD development [9,10].

One of the AD hypothesis is the cholinergic hypothesis [4,5,11] which has become the leading strategy for the development of cholinesterase inhibitors(ChEIs) aimed to increasing of levels of acetylcholine through inhibition of cholinesterases (ChEs) [12-14], since the cognitive and memory deterioration of AD is due to the low level of choline, especially ACh in the brain. The most prevailing hypothesis, the amyloid hypothesis posits that an increased production of β-amyloid peptide and its aggregation and accumulation in a brain lead to a neuronal cell death, cause the Aβ soluble oligomers and the assembly of Aβ aggregates into fibrils are toxic to neurons[6,14]. Another hypothesis was reported, it was suggested that oxidative stress is involved in the early stage of the pathologic cascade and represents a key factor to initiate the aggregation of β-amyloid and tau-protein hyperphosphorylation[15]. Accordingly, many antioxidants that specifically scavenge oxygen radicals were observed to be able to attenuate the syndrome of AD and prevent the progression of the disease[16]. In addition, another AD hypothesis called metal hypothesis indicates that the metals(Fe, Cu and Zn) also play a role in pathogenesis of AD [17]. It was observed that during disease progression from moderate to severe AD, the metals progressively accumulate in AD patients [18]. The abnormal accumulation of metals is closely associated with the formation of Aβ plaques and neurofibrillary tangles (NFT), the hallmarks in brain of AD patients [19, 20]. Besides, the abnormally high levels of Cu and Fe in brain catalyze the production of reactive oxygen species (ROS), which further elicit oxidative stress contributing to the AD pathogenesis [20-22]. Thus, lowering the concentration of metals in brain by chelating metals represents another rational therapeutic approach for halting AD pathogenesis.

Because of the multifactorial nature of AD as above mentioned, AD treating remains a challenge for the pharmaceutical community and no effective drug is currently available. There have been many approaches to potential therapies, most treatment strategies have aimed at cholinergic neurotransmission and β-amyloid peptide. However, cholinesterase inhibitors were the first and, to date, the only class of drugs in the market that showed some results in the treatment of AD (such as tacrine, donepezil, rivastigmine and galantamine, Fig. 1). As the traditional ‘one molecule, one target’ paradigm, the so-called magic bullets, can generally only offer limited and transient benefits, these drugs that modulate such a single target could only improve symptoms or enable a palliative treatment instead of curing or preventing the neurodegeneration, and exert limited effects on most patients[23]. It is unlikely that a unitary mechanism of action will provide a comprehensive therapeutic approach to such multifaceted neurodegenerativedisease. Thus, efficient therapy is more likely to be achieved by drugs that incorporate several pharmacological effects into a single molecular entity. This concept has been rationalized in the field of neurodegenerative diseases affording the multitarget-directed ligands (MTDLs) design strategy[24-27]. The strategy holds that single molecules being properly combined two or more distinct pharmacological properties and then able to act at

different targets in the neurodegenerative process, can achieve greater effectiveness compared to single-targeted drugs for investigating AD. Hence many studies have been devoted to the search for multifunctional agents that simultaneously inhibit cholinesterase, decrease Aβ levels and antioxidant[28, 29].

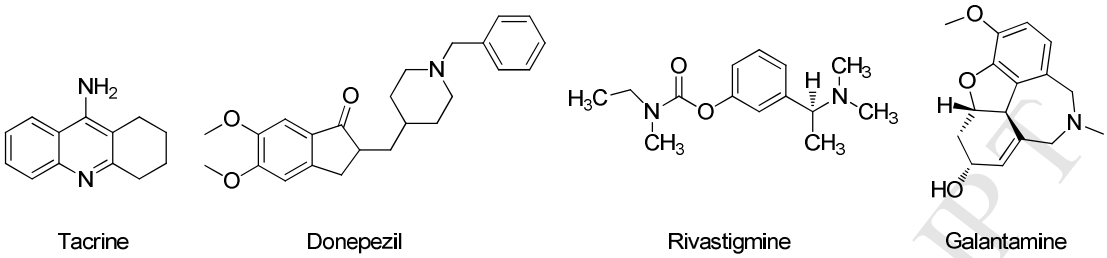

Figure 1. Chemical structure of reported AChE inhibitors

Tacrine was the first approved cholinesterase inhibitor by the FDA for the treatment of AD[30]. Although, its side effects, its modification is still of great interest. Recent studies have demonstrated that homo- and hetero-dimers can improve the biological profile of tacrine and even overcome some of its side effects[31]. Nevertheless, some of tacrine derivatives as hybrid potential drugs, have been developed to improve its activity[29], including tacrine-8-hydroxyquinoline[32], tacrine-fluorobenzoic acid[33] and tacrine-multialkoxybenzene hybrids[34]. Moreover, some studies have suggested that electron-rich aromatics would bind to the peripheral binding site, which have been confirmed in a comparison of aromatics with differing electron density[35]. Therefore development of tacrinehybrids that combines the ChEs inhibition, for the enhancement of the cholinergic neurotransmission, with reduction the Aβ fibril self-aggregation and antioxidant by conjugating with other active groups are attractive[36]. In order to further explore the anti-Alzheimer potential of the electron-rich aromatics based on MTDLs strategy, we herein reported a series of novel multifunctional compounds by conjugating a tacrine and electron-rich aromatics including benzoates, phenylacetates, cinnamates and acetylindole. A selection of these compounds were synthesized and evaluated for their in vitro activity as inhibitors of AChE, BuChE and self-induced Aβ aggregation activity.

2. Results and discussion

2.1. Chemistry

The tacrine-benzoates (or phenylacetates or cinnamates or acetylindole) hybrids were synthesized as shown in Scheme 1. Tacrine **4** was firstly prepared according to the literature with a total yield of 68.1% (see supporting information, scheme s1)[36]. It was then treated with bromoacetyl bromide in the presence of Et_3N to yield bromoacetylated intermediate **5** in a yield of 82.3%. Compound **5** was finally reacted with corresponding carboxylic acid derivatives **6a**-**6o** to afford the desired products **7a**-**7n**.

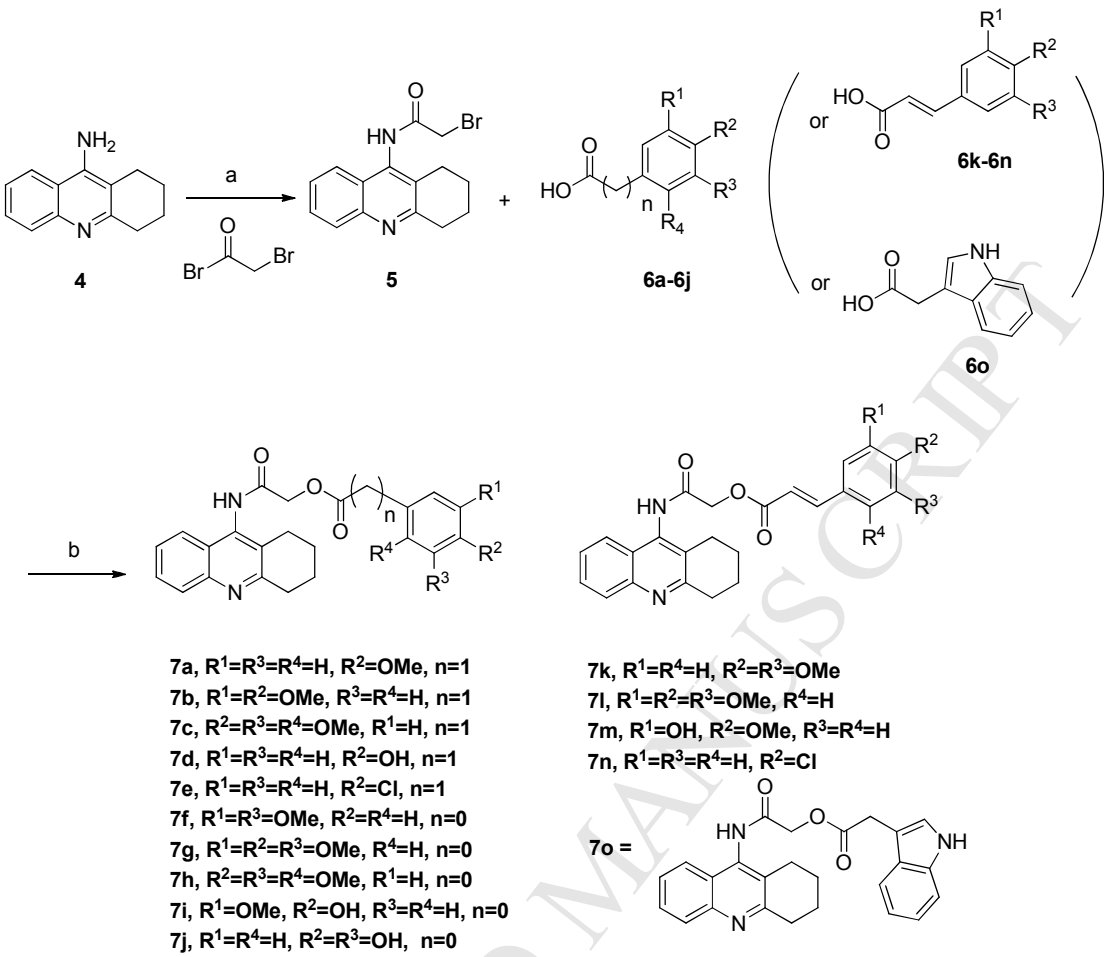

Scheme 1.Synthesis of tacrine-electron-rich aromatics hybrids. Reagents and conditions: (a) Et_3N, reflux; (b) DMF,K_2CO_3, rt.

2.2. In vitro inhibition studies on AChE and BuChE

To determine the potential of the target compounds **7a**-**7o** for the treatment of AD, their acetylcholinesterase (AChE, from *electric eel*) and butyrylcholinesterase (BuChE, from *equine serum*) inhibitory activities were determined by the method of Ellman et al[37], using tacrine as a reference compound. The IC_{50} values of all test compounds for ChEs (AChE and BuChE) and the affinity ratios were summarized as shown in Table 1.The results showed that most of the tested compounds (**7a**-**7o**) had significant ChEs inhibitory activity with IC_{50} values ranging from sub-micromolar to low nanomolar range. All synthesized compounds showed certain selectivity for AChE over BuChE and the ratio of BuChE/AChE affinity ranged from 1.2- to 64.6-fold. The compounds showed higher inhibitory potential against AChE that would possess higher BuChE/AChE affinity ratios.

Some of these new compounds have much more capability to inhibit AChE but all of these compounds unfortunatly showed weaker inhibitory activity for BuChE when compared to the reference drug, tacrine. Among these, compound **7c**, with a trimethoxyl phenylacetate group, showed the most potent inhibition for AChE with an

IC_{50} value of 5.63 nM, and the potency was 13-times stronger than the reference compound tacrine with IC_{50} value of 73.36 nM. The inhibition for BuChE with an IC_{50} value of 364 nM was weaker than AChE and the highest ratio of BuChE/AChE was also observed with affinity ratio value of 64.6. This result indicated that compound **7c** showed the highest selectivity for AChE over BuChE. Furthermore, a structure-activity relationship analysis suggested that the electron density of aromatic ring which was linked with tacrine through acetyl group played a significant role in determining the inhibitory activity for AChE in present work. When the aromatic ring bore more electron-donating substituents among the homogeneous class of compounds, the AChE inhibitory activity was increased. For instance, the homogeneous class of compounds **7a** and **7b** (n=1) with only one and two methoxy substituents respectively, exhibited relatively low AChE inhibitory activities compared with **7c**. Compound **7g**, which had trimethoxylbenzoate substituent similar to **7c**, appeared to be the third strong inhibitor with IC_{50} value of 8.46 nM. A similar result was attached by compound **7o** with an electron-rich indolyl moiety and it was a strong inhibitor with IC_{50} value of 8.13 nM. Compound **7g** and **7o** also exhibited the 2nd and 3rd high selectivity with affinity ratio values were 38.5 and 35.7 respectively. However, some decreased inhibitory activities for AChE were afforded from compounds **7b**, **7f** and **7k** with two methoxy substituents on the aromatic ring and all of them showed weak selectivity with affinity ratio values were 8.5, 14.3 and 9.8 respectively. In contrast, the weakest two inhibitory activities for AChE were obtained from compounds **7e** and **7n**, with IC_{50} values of 182.8 nM and 213.3 nM respectively. Both of them had a chloro group as electron-withdrawing substituent. The results revealed that the inhibitory activity for AChE could be drastic decreased with an electron-deficient moiety. In addition, it was observed that there was a slightly reduction of inhibitory activity for AChE of compound **7l** compared to **7c** and **7g**. Despite that the same electron-rich aromatic ring was afforded, the IC_{50} value for AChE of compound **7l** was raised to 16.88 nM. The possible reason of the result could be that the additional vinyl group enlarged the conjugated regions in the same substituents of aromatic ring, which meant the electron density of phenyl group was averaged and thus led to an electron-deficient effect. Furthermore, the linker length between tacrine and phenyl moiety affected the AChE inhibitory activity and selectivity as well. It was suggested that phenylacetate group (**7c**) was preferred to benzoate group (**7g**). Finally, the AChE inhibitory activities of all hydroxyl substituted derivatives were less than methoxy substituted derivatives, which indicated that methoxy moiety was superior to hydroxyl for inhibited AChE. The reason for this result could be hyperconjugation effect of methoxy group, which led to more potency electron-donating ability of methoxy group compared with hydroxyl group.

Table 1. Inhibition of ChEs activity, affinity ratios and inhibition of Aβ(1-42) self-induced aggregation

Compds	IC_{50}[a] for AChE (nM)	IC_{50}[a] for BuChE (nM)	Affinity ratios[b]	Aβ(1-42) aggregation[c] inhibition (nM)
7a	25.26±0.75	319.3±0.05	12.6	71.28±0.04

7b	65.07±0.23	554.1±0.05	8.5	22.54±0.01
7c	5.63±0.98	364±0.05	64.6	51.81±0.05
7d	73.96±2.44	238.8±0.03	3.2	45.29±0.03
7e	182.8±0.16	218.2±0.06	1.2	77.45±0.03
7f	15.69±1.19	223.5±0.04	14.3	55.86±0.04
7g	8.46±0.51	329.3±0.05	38.5	30.74±0.03
7h	15.46±0.56	254.8±0.05	16.4	65.50±0.03
7i	70.06±0.37	319±0.06	4.5	37.36±0.05
7j	132.85±0.90	344.4±0.06	2.6	17.36±0.03
7k	16.22±0.85	159.2±0.04	9.8	49.14±0.02
7l	16.88±0.47	298.9 ±0.03	17.9	45.88±0.02
7m	74.87±0.57	355 ±0.01	4.7	46.12±0.04
7n	213.34±0.38	541.7 ±0.05	2.5	51.77±0.02
7o	8.13±4.72	291.7 ±0.05	35.7	38.96±0.01
Tacrine	73.36±0.22	14.45 ±0.04	0.20	12.21±0.02

[a]AChE from *electric eel*, BuChE from *equine serum*; IC_{50}, inhibitor concentration (means±SEM of three experiments) for 50% inactivation of AChE.

[b] Affinity ratios = IC_{50} (BuChE)/IC_{50} (AChE)

[c]Inhibition of self-mediated Aβ(1-42) aggregation, the thioflavin-T fluorescence method was used, the mean±SD of at least three independent experiments and the measurements were carried out in the presence of 5, 10, 20, 50, 100 μM compounds respectively.

2.3. Kinetic characterization of ChEs inhibition

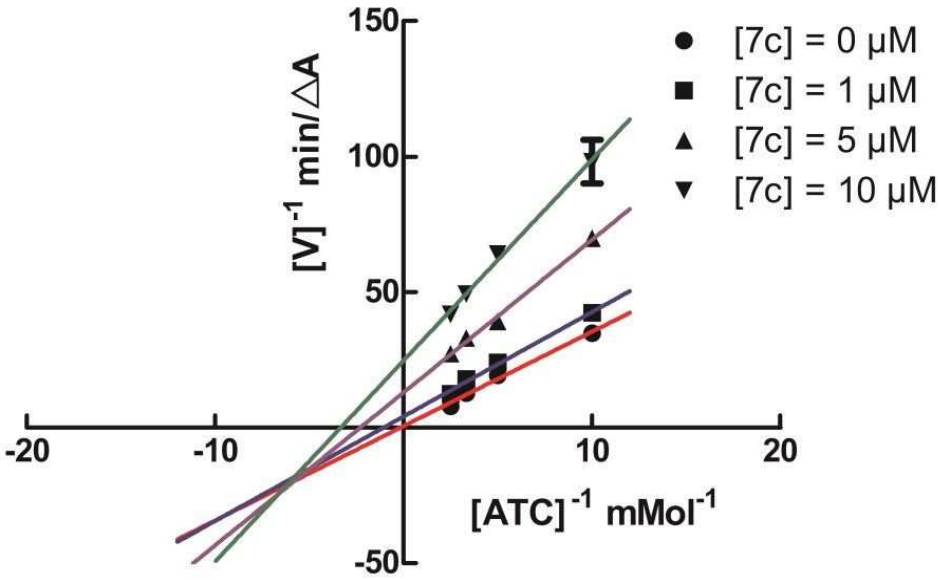

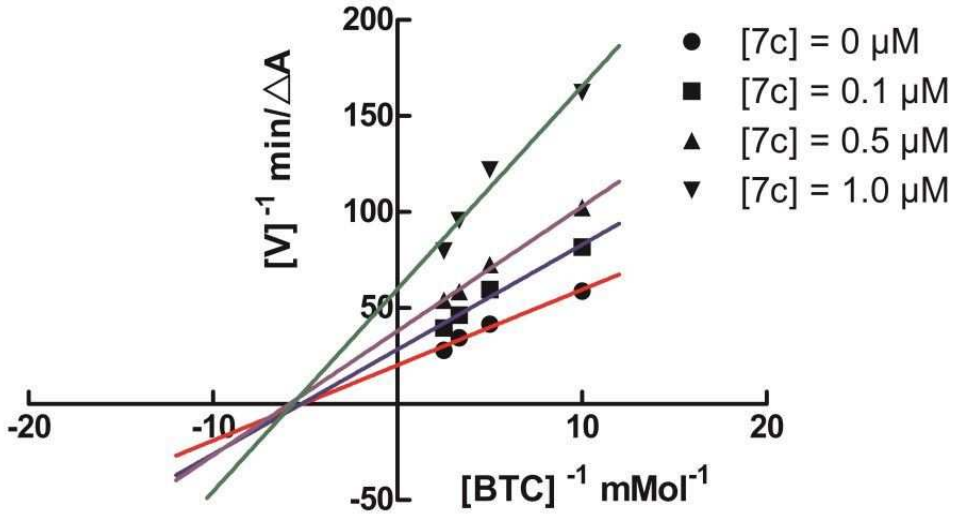

Figure 2. Lineweaver-Burk plot for compound **7c** with AChE and BuChE, respectively.

Because compounds **7c** was the best AChE inhibitor and a better BuChE inhibitor, it was selected for kinetic measurements by using graphical analysis of steady-state inhibition data in order to gain information about the mode of inhibition and binding of the novel inhibitors. As shown in Fig. 2, The Lineweaver-Burk plots for AChE showed reversible and a mixed type inhibition, which indicated that compounds **7c** could bind to both catalytic active site (CAS) and the peripheral anionic site (PAS) of AChE simultaneously. It had been reported that some amino acids in PAS of AChE could promote Aβ fibrillation, and an inhibitor of PAS, propidium, was able to block this activity [39,40]. Therefore, the inhibitors which could bind to both CAS and PAS of AChE might have dual inhibition for both AChE activity and AChE induced Aβ aggregation. A similar interaction was found between **7c** and BuChE by means of Lineweaver-Burk plot.

2.4. Inhibition of self-mediated Aβ(1-42) aggregation

All synthesized compounds were also tested for their ability to inhibit self-mediated aggregation of Aβ(1-42) by using a thioflavin T fluorescence method[38]. Tacrine was used as reference compound. From the results summarized in Table 1, it could be seen that these hybrids apparently prevented the self-mediated Aβ aggregation with IC_{50} ranging from 17.36 nM to 71.28 nM and showed a little less potencies relative to that of tacrine (12.21 nM). Compounds **7b**, **7c**, **7g** and **7o** having the high inhibitory activity for AChE also exhibited the good potency on inhibition of self-induced Aβ (1-42) aggregation with IC_{50} values of 22.54, 51.81 nM, 30.74 nM and 38.96 nM respectively, which were weaker than that of reference compound tacrine. Unfortunately, **7c** as the most potent AChE inhibitor only showed relatively moderate inhibitory potency, with an IC_{50} value of 51.81 nM. In contrast, compound **7j** with a

hyroxylbenzoate group unexpectedly showed the most potency with an IC_{50} value of 17.36 nM among all these compounds. These results indicated that hydroxyl moiety was superior to alkoxyl for inhibitory activity of Aβ (1-42) self-aggregation compared to inhibitory activity of AChE. Besides, different from AChE inhibition, the electron density of aromatic ring which was linked with tacrine through acetyl group and the linker length between tacrine and phenyl moiety were not important factors for inhibition of Aβ (1-42) self-aggregation. The relationship between them and the inhibitory activity was not clear. For instance, compounds **7e** and **7n** with chloro phenylacetate and chloro cinnamate as electron-withdrawing substituents, exhibited relatively low inhibitory activities with IC_{50} values of 77.45 and 51.77 nM, respectively. However, there were no significant changes in the inhibitory activities compared with the homogeneous class of compounds **7a** and **7k** with IC_{50} values of 71.28 and 49.14 nM, respectively.

2.5. Inhibition of Aβ(1-42) fibril formation monitored by transmission electron microscopy (TEM)

To further confirm the ability of synthesized compounds and tacrine in inhibiting Aβ(1-42) aggregation, the inhibitory activities of compounds **7b**, **7c** and tacrine were monitored by using TEM[41]. As shown in Fig. 3, after 24 h of incubation at 37°C, Aβ(1-42) alone aggregated into well-defined Aβ fibrils and amorphous deposits were observed for the sample of Aβ(1-42) alone (Fig. 3b). In contrast, no obvious Aβ fibril was observed in the presence of tacrine and compound **7b** (Fig. 3c, d) under identical conditions. Meanwhile, when compound **7c** was incubated with Aβ(1-42) under identical conditions, few short fibrils were found (Fig. 3e). These TEM experimental results were in agreement with the results of ThT studies, which further strongly proved that compound **7b** and tacrine could inhibit and slow down the Aβ(1-42) fibrils formation. Unfortunately, tacrine was the most potency inhibitory activity compared to other synthesized compounds.

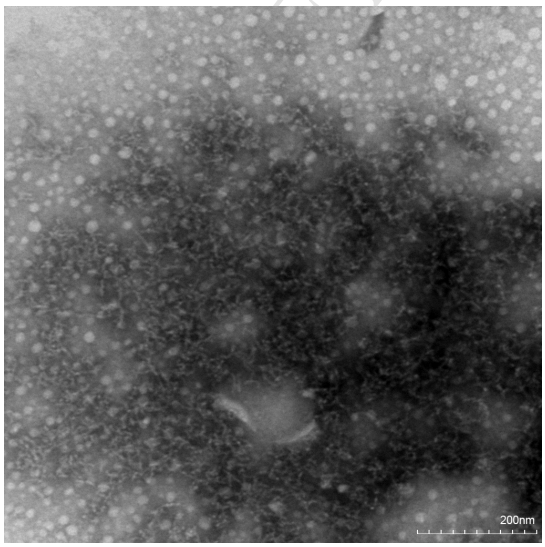

(a) Aβ alone (0h)

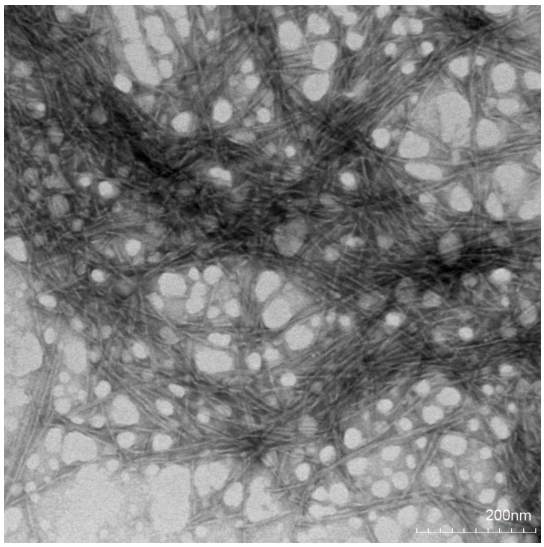

(b) Aβ alone (24h)

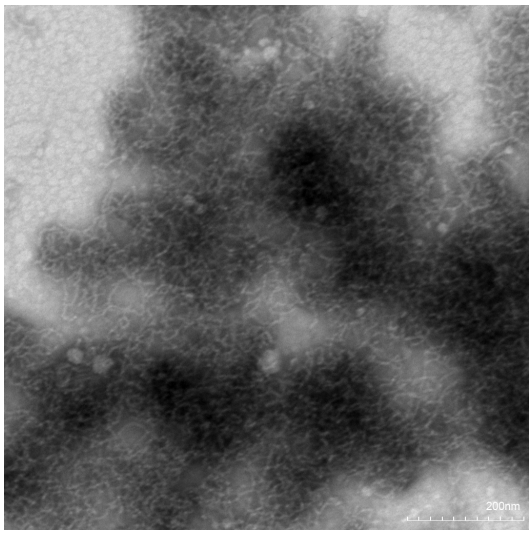

(c) Aβ+ Tacrine (24h)

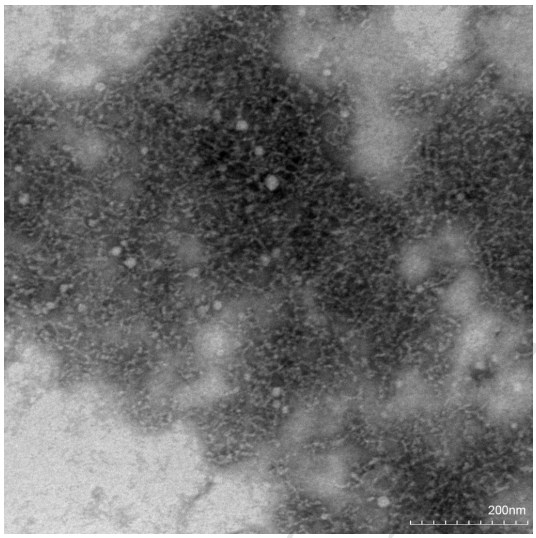

(d) Aβ+ **7b** (24h)

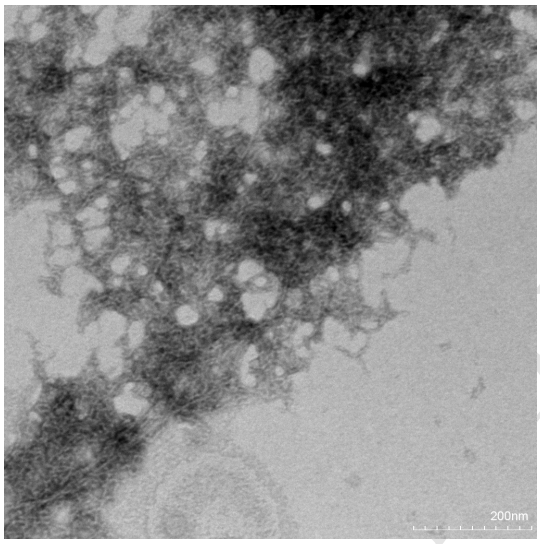

(e) Aβ+ **7c** (24h)

Figure 3. TEM image analysis of Aβ(1-42) aggregation. (a) Aβ(1-42) alone (20 μM) was incubated at 37 ^{o}C for 0 h (a) Aβ(1-42) alone (20 μM) was incubated at 37 ^{o}C for 24 h; (c) Aβ(1-42) (20 μM) and tacrine (50 μM) were incubated at 37 ^{o}C for 24 h; (c) Aβ(1-42) (20 μM) and **7b** (50 μM) were incubated at 37 ^{o}C for 24 h; (d) Aβ(1-42) (20 μM) and **7c** (50 μM) were incubated at 37 ^{o}C for 24 h

2.6. Molecular modeling study

Table 2. The Docking Cscore of **7c** and AchE/ BchE respectively

Compound	Cscore for AChE	Cscore for BChE	Ratio
7c	8.00（crash:-1.59）	6.90(crash:-2.63)	12.6

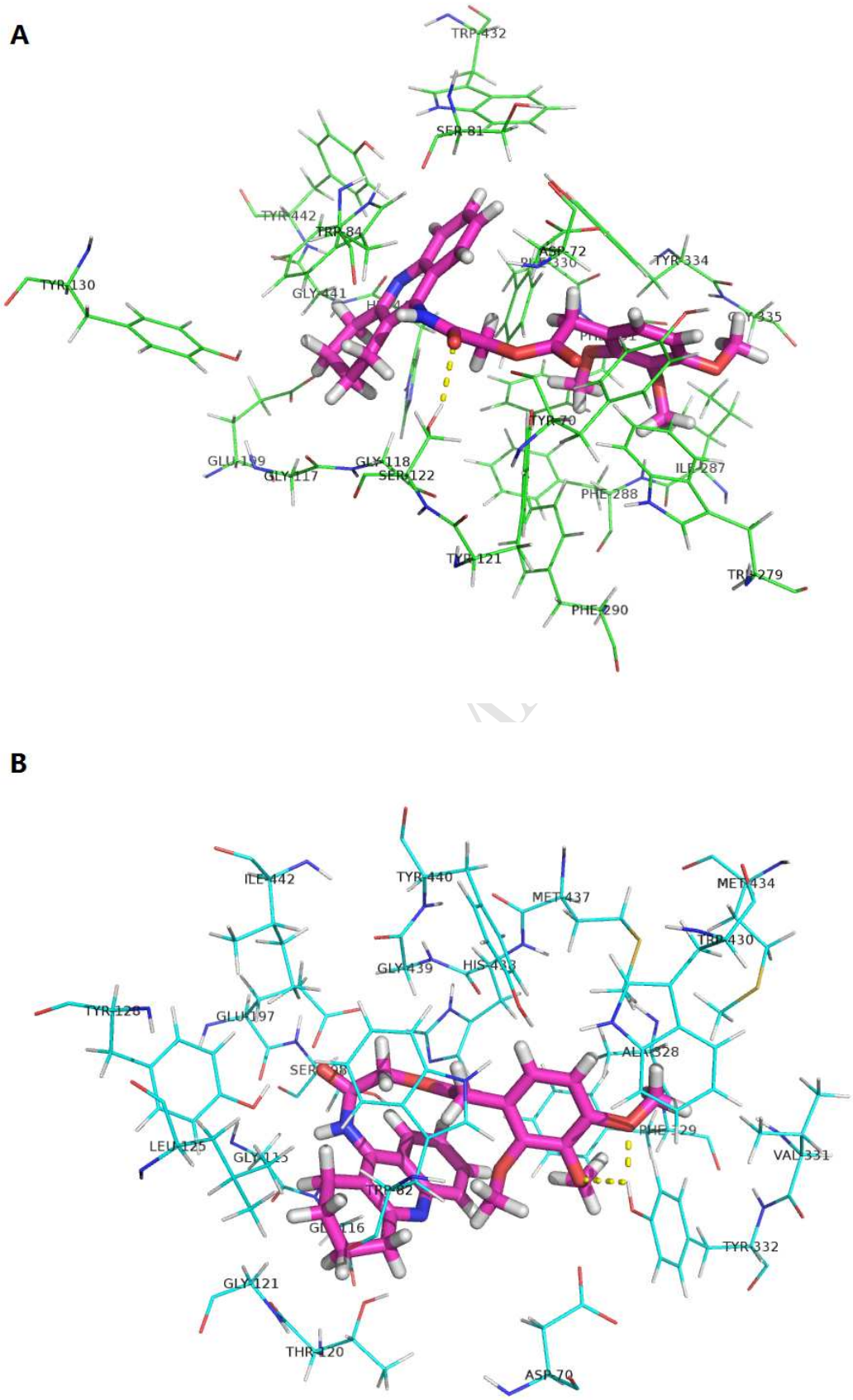

Figure 4. Molecular docking models of compound **7c** inside active site (3 Å) of AChE (A) and

BuChE (B).

To investigate the interaction mode of compound **7c** with *Tc*AChE (PDB code: 1ACJ) and *h*BuChE(PDB code：4BDS), molecular modeling was carried out by Sybyl_8.1.1 package with Surflex-Dock program as shown in Fig. 4. Their Cscores were calculated as shown in Table 2. As expected that AChE exhibited higher Cscore (8.00) while BuChE (6.90) which were consistent with the experimental result. Furthermore, Ser122 in AChE, and Tyr332 in BuChE were considered as the important residues which were reasonable for the binding mode of **7c** and AChE/ BuChE respectively. Meanwhile, there were several differences in the pocket between AChE and BuChE. Such as Trp84, Asp72, Tyr121, Gly118, Phe288, in AChE，and Asp70, Thr120 Val331, GLY116, ILE69, TYR332 in BuChE, and so on. These key amino residues around the binding pocket of AChE/BuChE, can influence charge in the active pocket conformation. Which indicated that, there was conformation difference of the same binding ligand. In another aspect, different substituted group in the main frame will get different selectivity of AChE/ BuChE. It was claimed that electron contributing group in R^1, R^2, R^3 and R^4 are facilited for AChE selectivity.

3. Conclusion

In summary, a series of tacrine - benzoates (or phenylacetates or cinnamates) hybrids have been designed, synthesized and evaluated as novel multi-potent anti-Alzheimer drug candidates. The results showed that most of these synthesized compounds had high ChEs and self-induced β-amyloid (Aβ) aggregation inhibitory potency in the nanomolar range *in vitro,* certain selectivity for AChE over BuChE with the ratio of BuChE/AChE selectivity ranged from 0.34- to 64.6- fold. Especially compound **7c**, with a trimethoxyl phenylacetate group, showed the most potent inhibition for AChE with an IC_{50} value of 5.63 nM, which was 13-times stronger than the reference compound tacrine and the highest selectivity (AChE / BuChE = 64.6). A Lineweaver-Burk plot and molecular modeling study showed that **7c** targeted both the CAS and PAS of ChEs. In inhibition of Aβ aggregation assay, compound **7j** exhibited the most potency inhibitory of self-induced Aβ aggregation. The electron density of aromatic ring which was linked with tacrine through acetyl group and the linker length between tacrine and phenyl moiety were important factors for inhibition of AChE but were less important for Aβ (1-42) self-aggregation. Altogether, the multifunctional effects of the new hybrids qualified them as potential anti-AD drug candidates, and compound **7c** might be considered as a promising lead compound for further research.

4. Experimental section

4.1. Chemistry

The ^{1}H NMR and ^{13}C NMR spectra were recorded using TMS as the internal standard on a Bruker Avnace III 400 spectrometer at 400 MHz and 100 MHz,

respectively. Coupling constants are given in Hz. High-resolution mass (HRMS) spectra were obtained with Shimazu LCMS-IT-TOF mass spectrometer. Mass spectra were recorded on a Agilent 6330 Ion Trap Mass Spectrometer. Reaction progress was monitored using analytical thin layer chromatography (TLC) on precoated silica gel GF254 (Qingdao Haiyang Chemical Plant, Qingdao, China) plates and the spots were detected under UV light (254 nm). Flash column chromatography was performed with silica gel (200-300 mesh) purchased from Qingdao Haiyang Chemical Co. Ltd or alumina from Sinopharm Chemical Reagent Co. Ltd. The purity of all compounds used for biological evaluation was confirmed to be higher than 95% through analytical HPLC performed with Agilent 1260 HPLC System (methol/water as eluent with a YMC ODS-A column, detected at UV 256 nM).

4.2. Synthesis of intermediate 5

A solution of bromoacetyl bromide (0.5 mL) in CH_2Cl_2 (10 mL) was added dropwise to an ice-cold solution of Et_3N (2.5 mmol, 1.8 mL) and tacrine **4** (1.0 g, 5.0 mmol) in CH_2Cl_2 (30 mL). After completed addition the solution was stirred for 2 h at room temperature. When the reaction was completed, it was diluted with CH_2Cl_2, washed with water, followed by brine solution. The organic layer was dried over anhydrous Na_2SO_4 and concentrated under reduced pressure. The obtained residue was purified bysilica gel chromatography using CH_2Cl_2/MeOH (100:1) as eluent to give compound **5** as a white solid. Yield: 82.3%. ^{1}H NMR (DMSO, 400MHz) δ(ppm): 10.14 (s, 1H), 8.04 (d, *J* = 8.3Hz, 1H), 7.80 (d, *J* = 8.5Hz, 1H), 7.66 (t, *J* = 7.6Hz, 1H), 7.52 (t, *J* = 7.7Hz, 1H), 4.20 (s, 2H), 3.18 (t, *J* = 6.5Hz, 2H), 2.85 (t, *J* = 6.4Hz, 2H), 1.95 – 1.74 (m, 4H). MS m/z$(M+H)^+$: 320.17.

4.3. General procedures for the preparation of 7a-7o

A solution of **5** (5.0mmol) in DMF (10 mL) was added dropwise to an ice-cold solution of a mixture of **6** (5.0mmol) and anhydrous potassium carbonate (5.0 mmol) in DMF (20 mL). After completed addition the solution was stirred for 2.5 h at room temperature. When the reaction was completed, it was diluted with H_2O, extracted with EtOAc three times (50 mL x 3), washed with water, followed by brine solution. The organic layer was dried over anhydrous Na_2SO_4 and concentrated under reduced pressure. The obtained residue was purified by silica gel chromatography.

4.3.1 2-oxo-2-((1,2,3,4-tetrahydroacridin-9-yl)amino)ethyl 2-(4-methoxyphenyl)acetate (7a)

Compound **5** was treated with 2-(4-methoxyphenyl) acetic acid (**6a**) according to general procedure to give the desired product **7a** as a white solid. Yield: 48.9%. ^{1}H NMR (DMSO, 400MHz) δ(ppm): 10.11 (s, 1H), 7.90 (d, *J* = 8.3 Hz, 1H), 7.86 (d, *J* = 8.3 Hz, 1H), 7.67 (t, *J* = 8.3 Hz, 1H), 7.50 (t, *J* = 8.1 Hz, 1H), 7.24 (d, *J* = 8.7 Hz, 2H), 6.90 (d, *J* = 8.7 Hz, 2H), 4.89 (s, 2H), 3.77 (s, 2H), 3.74 (s, 3H), 3.05 (t, *J* = 6.5 Hz, 2H), 2.74 (t, *J* = 6.3 Hz, 2H), 1.95 – 1.74 (m, 4H). ^{13}C NMR (100 MHz, DMSO)

δ(ppm): 171.92, 166.50, 159.82, 158.67, 146.76, 139.23, 131.00, 130.85, 129.21, 128.61, 128.00, 126.47, 126.06, 124.53, 123.74, 114.22, 114.10, 63.21, 55.49, 33.84, 25.16, 22.86, 22.43. ESI-HRMS Calcd. for $C_{24}H_{24}N_2O_4$ $[M+H]^+$: 405.1809; found: 405.1799.

4.3.2 2-oxo-2-((1,2,3,4-tetrahydroacridin-9-yl)amino)ethyl 2-(3,4-dimethoxyphenyl) acetate (7b)

Compound **5** was treated with 2-(3,4-dimethoxyphenyl) acetic acid (**6b**) according to general procedure to give the desired product **7b** as a white solid. Yield: 50.2%. ^{1}H NMR (400 MHz, DMSO) δ(ppm) :10.14 (s, 1H), 7.90 (d, *J* = 8.3 Hz, 1H), 7.85 (d, *J* = 8.2 Hz, 1H), 7.66 (t, *J* = 7.2 Hz, 1H), 7.49 (t, *J* = 7.2 Hz, 1H), 6.92 (dd, *J* = 8.2, 1.8 Hz, 1H), 6.88 (s, 1H), 6.83 (dd, *J* = 8.2, 1.8 Hz, 1H), 4.89 (s, 2H), 3.76 (s, 2H), 3.72 (s, 3H), 3.71 (s, 3H), 3.04 (t, *J* = 6.4 Hz, 2H), 2.73 (t, *J* = 6.3 Hz, 2H), 1.93 – 1.72 (m, 4H). ^{13}C NMR (100 MHz, DMSO) δ(ppm): 171.83, 166.51, 159.83, 148.96, 148.22, 146.78, 139.22, 129.20, 128.62, 128.00, 126.87, 126.04, 124.53, 123.73, 121.96, 113.65, 112.13, 63.22, 55.93, 55.83, 33.85, 25.17, 22.86, 22.43. ESI-HRMS Calcd. for $C_{25}H_{26}N_2O_5$ $[M+H]^+$: 435.1914; found: 435.1922.

4.3.3 2-oxo-2-((1,2,3,4-tetrahydroacridin-9-yl)amino)ethyl 2-(3,4,5-trimethoxyphenyl) acetate (7c)

Compound **5** was treated with 2-(3,4,5-trimethoxyphenyl)acetic acid (**6c**) according to general procedure to give the desired product **7c** as a white solid. Yield: 45.9%. ^{1}H NMR (DMSO, 400MHz) δ(ppm): 10.13 (s, 1H), 7.90 (d, *J* = 8.3 Hz, 1H), 7.87 (d, *J* = 8.4 Hz, 1H), 7.67 (t, *J* = 7.6 Hz, 1H), 7.50 (t, *J* = 7.6 Hz, 1H), 6.66 (s, 2H), 4.92 (s, 2H), 3.78 (s, 3H), 3.74 (s, 3H), 3.64 (s, 3H), 3.05 (t, *J* = 6.4 Hz, 2H), 2.75 (t, *J* = 6.3 Hz, 2H), 1.96 – 1.73 (m, 4H). ^{13}C NMR (100 MHz, DMSO) δ(ppm): 171.56, 166.49, 159.83, 153.16, 146.78, 139.20, 136.74, 130.17, 129.21, 128.63, 127.99, 126.03, 124.51, 123.72, 107.18, 63.28, 60.41, 56.21, 33.84, 25.18, 22.87, 22.43. ESI-HRMS Calcd. for $C_{26}H_{28}N_2O_6$ $[M+H]^+$: 465.2020; found: 465.2023.

4.3.4 2-oxo-2-((1,2,3,4-tetrahydroacridin-9-yl)amino)ethyl 2-(4-hydroxyphenyl)acetate (7d)

Compound **5** was treated with 2-(4-hydroxyphenyl)acetic acid (**6d**) according to general procedure to give the desired product **7d** as a white solid. Yield: 55.1%. ^{1}H NMR (400 MHz, DMSO) δ(ppm): 10.13 (s, 1H), 9.35 (s, 1H), 7.90 (d, *J* = 8.3 Hz, 1H), 7.85 (d, *J* = 8.1 Hz, 1H), 7.6 (t, *J* = 7.5 Hz, 1H), 7.50 (t, *J* = 7.5 Hz, 1H), 7.10 (d, *J* = 8.4 Hz, 2H), 6.71 (d, *J* = 8.5 Hz, 2H), 4.87 (s, 2H), 3.70 (s, 2H), 3.04 (t, *J* = 6.4 Hz, 2H), 2.73 (t, *J* = 6.3 Hz, 2H), 1.84 (m, 4H). ^{13}C NMR (100 MHz, DMSO) δ(ppm): 172.04, 166.52, 159.83, 156.74, 146.77, 139.23, 130.90, 129.19, 128.61, 128.01, 126.05, 124.65, 124.53, 123.74, 115.57, 63.19, 33.85, 25.16, 22.86, 22.43. ESI-HRMS Calcd. for $C_{23}H_{22}N_2O_4$ $[M+H]^+$: 391.1652; found: 391.1657.

4.3.5 2-oxo-2-((1,2,3,4-tetrahydroacridin-9-yl)amino)ethyl 2-(4-chlorophenyl)acetate (7e)

Compound **5** was treated with 2-(4-chlorophenyl)acetic acid (**6e**) according to general procedure to give the desired product **7e** as a white solid. Yield: 47.7%. ^{1}HNMR (DMSO, 400MHz) δ(ppm): 10.16 (s, 1H), 7.90 (d, *J* = 8.3 Hz, 1H), 7.85 (d, *J* = 8.2 Hz, 1H), 7.67 (t, *J* = 7.6 Hz, 1H), 7.50 (t, *J* = 7.5 Hz, 1H), 7.40 (d, *J* = 8.5 Hz, 2H), 7.35 (d, *J* = 8.5 Hz, 2H), 4.91 (s, 2H), 3.87 (s, 2H), 3.04 (t, *J* = 6.4 Hz, 2H), 2.73 (t, *J* = 6.3 Hz, 2H), 1.95 - 1.73 (m, 4H). ^{13}C NMR (DMSO, 100MHz) δ(ppm): 171.37, 166.39, 159.81, 146.76, 139.17, 133.66, 132.09, 131.90, 129.19, 128.74, 128.62, 127.99, 126.05, 124.50, 123.70, 63.33, 33.84, 25.16, 22.85, 22.42. ESI-HRMS Calcd. for $C_{23}H_{21}N_2O_3Cl$ $[M+H]^+$: 409.1313; found: 409.1311.

4.3.6 2-oxo-2-((1,2,3,4-tetrahydroacridin-9-yl)amino)ethyl 3,5-dimethoxybenzoate (7f)

Compound **5** was treated with 3,5-dimethoxybenzoic acid (**6f**) according to general procedure to give the desired product **7f** as a white solid. Yield: 42.4%. ^{1}H NMR (DMSO, 400MHz) δ(ppm): 10.25 (s, 1H), 7.92 (t, *J* = 9.1 Hz, 2H), 7.67 (t, *J* = 7.0 Hz, 1H), 7.53 (t, *J* = 7.2 Hz, 1H), 7.20 (d, *J* = 2.3 Hz, 2H), 6.83 (t, *J* = 2.3 Hz, 1H), 5.13 (s, 2H), 3.82 (s, 6H), 3.05 (t, *J* = 6.3 Hz, 2H), 2.80 (t, *J* = 6.2 Hz, 2H), 1.95 – 1.73 (m, 4H). ^{13}C NMR (DMSO, 100MHz) δ(ppm): 166.37, 165.75, 160.96, 159.83, 146.78, 139.25, 131.58, 129.20, 128.63, 127.95, 126.07, 124.51, 123.78, 107.56, 106.04, 63.80, 56.03, 33.85, 25.21, 22.87, 22.45. ESI-HRMS Calcd. for $C_{24}H_{24}N_2O_5$ $[M+H]^+$: 421.1715; found: 421.1761.

4.3.7 2-oxo-2-((1,2,3,4-tetrahydroacridin-9-yl)amino)ethyl 3,4,5-trimethoxybenzoate (7g).

Compound **5** was treated with 3,4,5-trimethoxybenzoic acid (**6g**) according to general procedure to give the desired product **7g** as a white solid. Yield: 57.8%. ^{1}H NMR (DMSO, 400MHz) δ(ppm): 10.24 (s, 1H), 7.93 (d, *J* = 8.4 Hz, 1H), 7.91 (d, *J* = 8.4 Hz, 1H), 7.67 (t, *J* = 8.2 Hz, 1H), 7.53 (t, *J* = 8.1 Hz, 1H), 7.36 (s, 2H), 5.13 (s, 2H), 3.86 (s, 6H), 3.76 (s, 3H), 3.05 (t, *J* = 6.4 Hz, 2H), 2.80 (t, *J* = 6.3 Hz, 2H), 1.95 – 1.75 (m, 4H). ^{13}C NMR (DMSO, 100MHz) δ(ppm): 166.44, 165.65, 159.84, 153.24, 146.78, 142.43, 139.25, 129.20, 128.63, 127.93, 126.06, 124.68, 124.51, 123.78, 107.23, 63.71, 60.67, 56.50, 33.85, 25.21, 22.87, 22.46. ESI-HRMS Calcd. for $C_{25}H_{26}N_2O_6$ $[M+H]^+$: 451.1864; found: 451.1868.

4.3.8 2-oxo-2-((1,2,3,4-tetrahydroacridin-9-yl)amino)ethyl 2,3,4-trimethoxybenzoate (7h)

Compound **5** was treated with 2,3,4-trimethoxybenzoic acid (**6h**) according to general procedure to give the desired product **7h** as a white solid. Yield: 45.2%. ^{1}H NMR ($CDCl_3$, 400MHz) δ(ppm): δ 8.85 (s, 1H), 8.03 (d, *J* = 8.5 Hz, 1H), 7.82 (d, *J* = 8.3 Hz, 1H), 7.71 (d, *J* = 8.8 Hz, 1H), 7.65 (t, *J* = 7.6 Hz, 1H), 7.48 (t, *J* = 7.6 Hz, 1H), 6.80 (d, *J* = 8.9 Hz, 1H), 5.14 (s, 2H), 3.94 (s, 3H), 3.93 (s, 3H), 3.81 (s, 3H), 3.18 (t, *J* = 6.3 Hz, 2H), 2.87 (t, *J* = 6.0 Hz, 2H), 1.93 – 1.72 (m, 4H). ^{13}C NMR (DMSO, 100MHz) δ(ppm): 166.64, 164.76, 159.83, 157.68, 154.67, 146.78, 142.86, 139.30, 129.18, 128.61, 127.93, 127.39, 126.03, 124.50, 123.83, 117.13, 108.20, 63.34, 62.17,

61.06, 56.57, 33.85, 25.23, 22.87, 22.45. ESI-HRMS Calcd. for $C_{25}H_{26}N_2O_6$ $[M+H]^+$: 451.1864; found: 451.1868.

4.3.9 2-oxo-2-((1,2,3,4-tetrahydroacridin-9-yl)amino)ethyl 3-hydroxy-4-methoxybenzoate (7i)

Compound **5** was treated with 3-hydroxy-4-methoxybenzoic acid (**6i**) according to general procedure to give the desired product **7i** as a white solid. Yield: 42.6%. ^{1}HNMR (DMSO, 400MHz) δ(ppm): 10.23 (s, 1H), 10.08 (s, 1H), 7.91 (t, *J* = 8.3, 2H), 7.67 (t, *J* = 8.2 Hz, 1H), 7.60 (dd, *J* = 8.3, 1.9 Hz, 1H), 7.56 – 7.49 (m, 2H), 6.91 (d, *J* = 8.3 Hz, 1H), 5.07 (s, 2H), 3.84 (s, 3H), 3.04 (t, *J* = 6.3 Hz, 2H), 2.79 (t, *J* = 6.2 Hz, 2H), 1.93 – 1.73 (m, 4H). ^{13}C NMR (DMSO, 100MHz) δ(ppm): 166.72, 165.88, 159.83, 152.32, 147.83, 146.77, 139.34, 129.18, 128.61, 127.96, 126.05, 124.55, 124.48, 123.82, 120.38, 115.68, 113.24, 63.34, 56.10, 33.85, 25.21, 22.87, 22.46. ESI-HRMS Calcd. for $C_{23}H_{22}N_2O_5$ $[M+H]^+$: 407.1601; found: 407.1601.

4.3.10 2-oxo-2-((1,2,3,4-tetrahydroacridin-9-yl)amino)ethyl 3,4-hydroxybenzoate (7j)

Compound **5** was treated with 3, 4-dihydroxybenzoic acid (**6j**) according to general procedure to give the desired product **7j** as a white solid. Yield: 40.4%. ^{1}H NMR (DMSO, 400MHz) δ(ppm): 10.26 (s, 1H), 9.71 (s, 2H), 7.91 (t, *J* = 7.7 Hz, 2H), 7.67 (t, *J* = 7.6 Hz, 1H), 7.53 (t, *J* = 7.6 Hz, 1H), 6.93 (d, *J* = 2.2 Hz, 2H), 6.48 (t, *J* = 2.2 Hz, 1H), 5.08 (s, 2H), 3.04 (t, *J* = 6.3 Hz, 2H), 2.78 (t, *J* = 6.2 Hz, 2H), 1.95 – 1.72 (m, 4H). ^{13}C NMR (DMSO, 100MHz) δ(ppm): 166.51, 166.15, 159.83, 159.02, 146.76, 139.32, 131.31, 129.20, 128.59, 127.95, 126.05, 124.51, 123.80, 107.93, 63.53, 33.84, 25.22, 22.87, 22.45. ESI-HRMS Calcd. for $C_{22}H_{20}N_2O_5$ $[M+H]^+$: 393.1445; found: 393.1451.

4.3.11 (*E*)-2-oxo-2-((1,2,3,4-tetrahydroacridin-9-yl)amino)ethyl 3-(3,4-dimethoxyphenyl)acrylate (7k)

Compound **5** was treated with (*E*)-3-(3,4-dimethoxyphenyl)acrylic acid (**6k**) according to general procedure to give the desired product **7k** as a pale yellow solid. Yield: 48.6%. ^{1}H NMR (DMSO, 400MHz) δ(ppm): 10.21 (s, 1H), 7.91 (dd, *J* = 8.4, 2.6 Hz, 2H), 7.72 (d, *J* = 16.0 Hz, 1H), 7.67 (t, *J* = 7.7 Hz, 1H), 7.52 (t, *J* = 7.5 Hz, 1H), 7.40 (d, *J* = 1.6 Hz, 1H), 7.29 (dd, *J* = 8.3, 1.6 Hz, 1H), 7.00 (d, *J* = 8.4 Hz, 1H), 6.70 (d, *J* = 16.0 Hz, 1H), 4.99 (s, 2H), 3.81 (s, 3H), 3.80 (s, 3H), 3.05 (t, *J* = 6.4 Hz, 2H), 2.78 (t, *J* = 6.2 Hz, 2H), 1.96 – 1.73 (m, 4H). ^{13}C NMR (DMSO, 100MHz) δ(ppm): 166.79, 166.73, 159.83, 151.60, 149.44, 146.77, 146.06, 139.34, 129.19, 128.60, 128.00, 127.23, 126.04, 124.55, 123.80, 123.67, 115.38, 111.96, 110.82, 62.95, 56.07, 56.02, 33.84, 25.20, 22.87, 22.46. ESI-HRMS Calcd. for $C_{26}H_{26}N_2O_5$ $[M+H]^+$: 447.1914; found: 447.1918.

4.3.12 (*E*)-2-oxo-2-((1,2,3,4-tetrahydroacridin-9-yl)amino)ethyl 3-(3,4,5-trimethoxyphenyl)acrylate (7l)

Compound **5** was treated with (*E*)-3-(3,4,5-trimethoxyphenyl)acrylic acid (**6l**)

according to general procedure to give the desired product **7l** as a pale yellow solid. Yield: 43.1%.[1]H NMR (DMSO, 400MHz) δ(ppm): 10.23 (s, 1H), 7.91 (dd, *J* = 8.2, 3.8 Hz, 2H), 7.73 (d, *J* = 16.0 Hz, 1H), 7.67 (t, *J* = 7.5 Hz, 1H), 7.52 (t, *J* = 7.5 Hz, 1H), 7.13 (s, 2H), 6.81 (d, *J* = 16.0 Hz, 1H), 5.00 (s, 2H), 3.82 (s, 6H), 3.70 (s, 3H), 3.05 (t, *J* = 6.3 Hz, 2H), 2.78 (t, *J* = 6.1 Hz, 2H), 1.95 – 1.75 (m, 4H). ^{13}C NMR (DMSO, 100MHz) δ(ppm): 166.64, 159.84, 153.56, 146.78, 146.06, 140.02, 139.31, 130.03, 129.19, 128.62, 127.99, 126.04, 124.54, 123.79, 117.24, 106.50, 63.03, 60.57, 56.50, 33.85, 25.21, 22.88, 22.46. ESI-HRMS Calcd. for $C_{27}H_{28}N_2O_6$ $[M+H]^+$: 477.2020; found: 477.2014.

4.3.13 (*E*)-2-oxo-2-((1,2,3,4-tetrahydroacridin-9-yl)amino)ethyl 3-(3-hydroxy-4-methoxyphenyl)acrylate (7m)

Compound **5** was treated with (*E*)-3-(3-hydroxy-4-methoxyphenyl)acrylic acid (**6m**) according to general procedure to give the desired product **7m** as a pale yellow solid. Yield: 52.6%. ^{1}H NMR (DMSO, 400MHz) δ(ppm): 10.19 (s, 1H), 9.69 (s, 1H), 7.90 (d, *J* = 8.5 Hz, 2H), 7.68 (d, *J* = 15.8 Hz, 1H), 7.67 – 7.64 (m, 1H), 7.52 (t, *J* = 7.5 Hz, 1H), 7.37 (d, *J* = 1.5 Hz, 1H), 7.17 (dd, *J* = 8.2, 1.5 Hz, 1H), 6.81 (d, *J* = 8.2 Hz, 1H), 6.62 (d, *J* = 15.9 Hz, 1H), 4.97 (s, 2H), 3.82 (s, 3H), 3.05 (t, *J* = 6.3 Hz, 2H), 2.78 (t, *J* = 6.2 Hz, 2H), 1.93 – 1.75 (m, 4H). ^{13}C NMR (DMSO, 100MHz) δ(ppm): 166.89, 166.78, 159.83, 150.01, 148.41, 146.78, 146.41, 139.34, 129.18, 128.61, 128.00, 126.03, 125.98, 124.56, 123.82, 116.00, 114.29, 111.72, 62.90, 56.15, 33.85, 25.20, 22.88, 22.46. ESI-HRMS Calcd. for $C_{25}H_{24}N_2O_5$ $[M+H]^+$: 433.1758; found: 433.1755.

4.3.14 (*E*)-2-oxo-2-((1,2,3,4-tetrahydroacridin-9-yl)amino)ethyl 3-(4-chlorophenyl)acrylate (7n)

Compound **5** was treated with (*E*) -3-(4-chlorophenyl)acrylic acid (**6n**) according to general procedure to give the desired product **7n** as a white solid. Yield: 49.5%. ^{1}H NMR (DMSO, 400MHz) δ(ppm): 10.18 (s, 1H), 7.90 (d, *J* = 8.4 Hz, 2H), 7.84 – 7.73 (m, 3H), 7.67 (t, *J* = 7.7 Hz, 1H), 7.55 – 7.47 (m, 3H), 6.81 (d, *J* = 16.0 Hz, 1H), 5.00 (s, 2H), 3.04 (t, *J* = 6.3 Hz, 2H), 2.78 (t, *J* = 6.2 Hz, 2H), 1.95 – 1.75 (m, 4H). ^{13}C NMR (DMSO, 100MHz) δ(ppm): 166.56, 166.36, 159.82, 144.42, 135.66, 133.39, 130.69, 129.50, 129.25, 128.55, 128.00, 126.09, 124.52, 123.79, 118.79, 63.14, 33.80, 25.19, 22.85, 22.44. ESI-HRMS Calcd. for $C_{24}H_{21}N_2O_3Cl$ $[M+H]^+$: 421.1313; found: 421.1305.

4.3.15 2-oxo-2-((1,2,3,4-tetrahydroacridin-9-yl)amino)ethyl 2-(1H-indol-3-yl)acetate (7o)

Compound **5** was treated with 2-(1H-indol-3-yl)acetic acid (**6o**) according to general procedure to give the desired product **7o** as a white solid. Yield: 43.5%, ^{1}H NMR (DMSO, 400MHz) δ(ppm): 10.97 (s, 1H), 10.12 (s, 1H), 7.89 (dd, *J* = 8.3, 7.7 Hz 2H), 7.67 (t, *J* = 7.6 Hz, 1H), 7.55 (d, *J* = 7.8 Hz, 1H), 7.50 (t, *J* = 7.6 Hz, 1H), 7.37 (d, *J* = 8.1 Hz, 1H), 7.32 (d, *J* = 2.3 Hz, 1H), 7.09 (t, *J* = 7.5 Hz, 1H), 6.98 (t, *J* =

7.5 Hz, 1H), 4.90 (s, 2H), 3.93 (s, 2H), 3.05 (t, *J* = 6.5 Hz, 2H), 2.75 (t, *J* = 6.3 Hz, 2H), 1.97 – 1.70 (m, 4H). ^{13}C NMR (DMSO, 100MHz) δ(ppm): 172.01, 166.65, 159.83, 146.75, 139.28, 136.56, 129.21, 128.59, 128.03, 127.60, 126.06, 124.73, 124.54, 123.77, 121.57, 119.08, 118.96, 111.88, 107.17, 63.17, 33.84, 30.85, 25.18, 22.87, 22.44. ^{13}C NMR(DMSO, 100MHz) δ(ppm): 172.01, 166.65, 159.83, 146.75, 139.28, 136.56, 129.21, 128.59, 128.03, 127.60, 126.06, 124.73, 124.54, 123.77, 121.57, 119.08, 118.96, 111.88, 107.17, 63.17, 33.84, 30.85, 25.18, 22.87, 22.44. ESI-HRMS Calcd. for $C_{25}H_{23}NO_3$ $[M+H]^+$: 414.1812; found: 414.1799.

4.4. Biological activity

4.4.1. *In vitro* inhibition studies on AChE and BuChE

Acetylcholinesterase (AChE, E.C. 3.1.1.7, from *electric eel*), butyrylcholinesterase (BuChE, E.C. 3.1.1.8, from *equine serum*), 5, 5'-dithiobis-(2-nitrobenzoic acid) (Ellman's reagent, DTNB), acetylthiocholinechloride (ATC), butylthiocholine chloride (BTC), and tacrine hydrochloride were purchased from Sigma Aldrich. Tacrine and synthesized derivatives were dissolved in DMSO (5‰) and fetal bovine serum(1‰), and then diluted in 0.1 M NaH_2PO_4/Na_2HPO_4 buffer (pH 7.4) to provide a final concentration range.

All the assays were under 0.1 M NaH_2PO_4/Na_2HPO_4 buffer, pH 7.4,using a THERMO Enzyme-labeled Instrument. Enzyme solutions were prepared to give 2.0 units/mL in 2 mL aliquots. The assay medium contained phosphate buffer, pH 7.4 (1 mL), 30 μL of 0.01 M DTNB, 10 μL of enzyme, and 30 μL of 0.01 M substrate (acetylthiocholine chloride). The substrate was added to the assay medium containing enzyme, buffer, and DTNB with inhibitor after 20 min of incubation time. The activity was determined by measuring the increase in absorbance at 410 nm at 1 min intervals at 37^{o}C. Calculations were performed according to the method of the equation in Ellman et al. Each concentration was assayed in triplicate.

In vitro BuChE assays were carried out using a similar method as described above.

4.4.2. Inhibition of self-mediated Aβ(1-42) aggregation

In order to investigate the self-mediated Aβ(1-42) aggregation, a thioflavin-T fluorescence assay was performed. Experiments were performed by incubating the peptides in 10 mM phosphate buffer (pH 7.4) at 37^{o}C for 24 h (final Aβ(1-42) 20 μM) with and without the tested compounds at different concentrations (5, 10, 20, 50 ,100 μM). After incubation, the samples were diluted to a final volume of 150 μL with 50 mM glycine-NaOH buffer (pH 8.5) containing 5 μM Thioflavin T. Fluorescence signal was measured (excitation wavelength 450 nm, emission wavelength 485 nm and slit widths set to 5 nm) on a Varioskan Flash Multimode Reader (Thermo Scientific). The percentage of inhibition on aggregation was calculated by the following expression: (1- IFi/IFc)*100% in which IFi and IFc were the fluorescence

intensities obtained for absorbance in the presence and absence of inhibitors, respectively, after subtracting the background fluorescence of the 5 μM Thioflavin T solution. Each measurement was run in triplicate.

4.4.3. Transmission electron microscopy (TEM) assay

Microscopy images were captured on HITACHI H-7650 transmission electron microscope. Aβ(1-42) peptide (Sigma) stock was diluted with 10 mM phosphate buffer (pH 7.4) at 4^{o}C to 100 μM before use. For the inhibition of self-induced Aβ(1-42) aggregation experiment, it was incubated in the presence and absence of compounds and tacrine at 37^{o}C for 24 h. Then, the 250 μM tested compound was added and incubated at 37^{o}C for another 24 h. The final concentrations of Aβ(1-42) was 20 μM and the compounds were 50 μM. Aliquots (5 uL) of the samples were placed on a carboncoated copper/rhodium grid for 2 min at room temperature. Each grid was stained with phosphomolybdic acid solution (3%, 5 uL) for 2 min. Excess staining solution was removed and the specimen was transferred for imaging with transmission electron microscopy.

4.5. Molecular modeling

For the docking studies, Surflex-Dock in Sybyl 8.1.1 was used. The structures of the inhibitors were drawn in the Sybyl package with standard bond lengths and angles, and minimized using the conjugate gradient method. The Gasteiger-Huckel charge was applied for the minimization process, with a distance-dependent dielectric function. A preliminary docking study was carried out using the crystal structure of *Tc*AChE (PDB code: 1ACJ) and *h*BuChE(PDB code：4BDS), The structure was polished as follows: all water molecules were removed from the crystal structure and the ligand was extracted. The AChE and BuChE proteins were then analyzed using the Protein Structure Preparation Tool in Sybyl. After adding hydrogens, the side-chain amides were also fixed and two bumping amino acids were adjusted. Stage minimization was also applied with the AMBER FF99 force field. Then the Protomol was generated.

Acknowledgements

We thank the Foundation of Educational Commission of Guangdong Province of China (Nos. 2013KJCX0151, 2014KTSCX096) for financial support of this study.

References

[1] D. J. Selkoe, Alzheimer’s Disease. Cold Spring Harbor Perspectives in Biology. 2011;3(7):a004457. doi:10.1101/cshperspect.a004457.

[2] L. Piazzi, A. Rampa, A. Bisi, S. Gobbi, F. Belluti, A. Cavalli, M. Bartolini, V. Andrisano , P. Valenti, M. Recanatini, J. Med. Chem. 46 (2003**)** 2279-2282.

[3] H. Tang, H. T. Zhao, S. M. Zhong, Z. Y. Wang, Z. F. Chen, H. Liang, Bioorg. Med.

Chem. Lett. 22 (2012) 2257-2261.
[4] A. V. Terry Jr, J. J. Buccafusco, J. Pharmacol. Exp. Ther. 306 (2003) 821-827.
[5] F. Gualtieri, S. Dei, D. Manetti, M. N. Romanelli, S. Scapecchi, E. Teodori, II Farmaco. 50 (1995) 489-503.
[6] J. Hardy, *J.* Neurochem. 110 (2009) 1129-1134.
[7] C. X. Gong, K. Iqbal, Curr. Med. Chem. 15 (2008) 2321-2328.
[8] K. M. Webber, A. K. Raina, M. W. Marlatt, X. Zhu, M. I. Prat, L. Morelli, G. Casadesus, G. Perry, M. A. Smith, Mech. Ageing. Dev. 126 (2005) 1019-1025.
[9] V. Tumiatti, A. Minarini, M.L. Bolognesi, A. Milelli, M. Rosini, C. Melchiorre, Curr. Med. Chem. 17 (2010) 1825-1838.
[10] E. Scarpini, P. Scheltens, H. Feldman, Lancet Neurol. 2 (2003) 539-547.
[11] D. Muñoz-Torrero, P. Camps, Curr. Med. Chem. 13 (2006) 399-422.
[12] D. Muñoz-Torrero, Curr. Med. Chem. 15 (2008) 2433-2455.
[13] S. Rizzo, C. Riviere, L. Piazzi, A. Bisi, S. Gobbi, M. Bartolini, V. Andrisano, F. Morroni, A. Tarozzi, J. P. Monti, A. Rampa, J. Med. Chem. 51 (2008) 2883-2886.
[14] J. Hardy, D. J. Selkoe, Science. 297 (2002) 353-356.
[15] A. Nunomura, R. J. Castellani, X. Zhu, P. I. Moreira, G. Perry, M. A. Smith, J. Neuropathol. Exp. Neurol. 65 (2006) 631-641.
[16] Q. Liu, F. Xie, R. Rolston, P. I. Moreira, A. Nunomura, X. Zhu, M. A. Smith, G. Perry, Mini-Rev. Med. Chem. 7 (2007) 171-180.
[17] A. I. Bush, R. E. Tanzi, Neurotherapeutics. 5 (2008) 421-432.
[18] P. Zatta, D. Drago, S. Bolognin, S. L. Sensi, Trends. Pharmacol. Sci. 30 (2009) 346-355.
[19] K. J. Barnham, A. I. Bush, Curr. Opin. Chem. Biol. 12 (2008) 222-228.
[20] A. I. Bush, J. Alzheimer's Dis. 15 (2008) 223-240.
[21] T. Amit, Y. Avramovich-Tirosh, M. B. Youdim, S. Mandel, FASEB J. 22 (2008) 1296-1305.
[22] H. Zheng, M. B. Youdim, M. Fridkin, J. Med. Chem. 52 (2009) 4095-4098.
[23] Y. Chen, J. Sun, L. Fang, M. Liu, S. Peng, H. Liao, J. Lehmann, Y. Zhang, J. Med. Chem. 55 (2012) 4309-4321.
[24] R. León, A. G. García, J. Marco-Contelles, Med. Res. Rev. 33 (2013) 139-189.
[25] M. Bajda, N. Guzior, M. Ignasik, B. Malawska, Curr. Med. Chem. 18 (2011) 4949-4975.
[26] (a) M. L. Bolognesi, E. Simoni, M. Rosini, A. Minarini, V. Tumiatti, C. Melchiorre, Curr. Top. Med. Chem. 11 (2011) 2797-2806. (b) M. L. Bolognesi, A. Minarini, M. Rosini, V. Tumiatti, C. Melchiorre, Mini-Rev. Med. Chem. 8 (2008) 960-967.
[27] L. Pisani, M. Catto, F. Leonetti, O. Nicolotti, A. Stefanachi, F. Campagna, A Carotti, Curr. Med. Chem. 18 (2011) 4568-4587
[28] (a) A. Cavalli, M. L. Bolognesi, A. Minarini, M. Rosini, V. Tumiatti, M. Recanatini, C. Melchiorre, J. Med. Chem. 51 (2008) 347-372. (b) M. Catto, A. A. Berezin, D. L. Re, G. Loizou, M. Demetriades, A. D. Stradis, F. Campagna, P. A. Koutentis, A. Carotti, Eur. J. Med. Chem. 58 (2011) 84-97.
[29] (a) A. Romero, R. Cacabelos, M. J. Oset-Gasque, A. Samadi, J. Marco-Contelles,

Bioorg. Med. Chem. Lett. 23 (2013) 1916-1922. (b) M. Khoobi, M. Alipour, Moradi, A.; A. Sakhteman, H. Nadri, S. F. Razavi, M. Ghandi, A. Foroumadi, A. Shafiee, Eur. J. Med. Chem. 68 (2013) 291-300. (c) M. Khoobi, F. Ghanoni, H. Nadri, A. Moradi, M. P. Hamedani, F. H. Moghadam, S. Emami, M. Vosooghi, R. Zadmard, A. Foroumadi, A. Shafiee, Eur. J. Med. Chem. 89 (2015) 296-303. (d) M. Tonelli, M. Catto, B. Tasso, F. Novelli, C. Canu, G. Iusco, L. Pisani, A. D. Stradis, N. Denora, A. Sparatore, V. Boido, A. Carotti, F. Sparatore, ChemMedChem 10 (2015) 1040-1053.

[30] E. Giacobini, Neurochem. Int. 32 (1998) 413-419. (e) J. L. Domínguez, F. Fernández-Nieto, M. Castro, M. Catto, M. R. Paleo, S. Porto, F. J. Sardina, J. M. Brea, A. Carotti, M. C. Villaverde, F. Sussman, J. Chem. Inf. Model, 55 (2015**)** 135–148.

[31] V. Tumiatti, A. Minarini, M. L. Bolognesi, A. Milelli, M. Rosini, C. Melchiorre, Curr. Med. Chem. 17 (2010) 1825-1838.

[32] M. I. Fernández-Bachiller, C. Pérez, G. C. González-Munoz, S. Conde, M. G. López, M. Villarroya, A. G. García, M. I. Rodríguez-Franco, J. Med. Chem. 53 (2010) 4927-4937.

[33] P. Szymanski, A. Karpinski, E. Mikiciuk-Olasik, Eur. J. Med. Chem. 46 (2011) 3250-3257.

[34] W. Luo, Y. P. Li, Y. He, S. L. Huang, D. Li, L. Q. Gu, Z. S. Huang, Eur. J. Med. Chem. 46 (2011) 2609-2616.

[35] (a) P. W. Elsinghorst, C. M. Tanarro, M. Gutschow, J. Med. Chem. 49 (2006) 7540-7544. (b) G. Ucar, N. Gokhan, A. Yesilada, A. A. Bilgin, Neurosci. Lett. 382 (2005) 327-331. (c) H. Nadri, M. Pirali-Hamedani, M. Shekarchi, M. Abdollahi, V. Sheibani, M. Amanlou, A. Shafiee, A. Foroumadi, Bioorg. Med. Chem. 18 (2010) 6360-6366.

[36] (a) S.-S. Xie, X. Wang, N. Jiang, W. Yu, K. D. G. Wang, J.-S. Lan, Z.-R. Li, L.-Y. Kong, Eur. J. Med. Chem. 95 (2015) 153-165. (b) S.-S. Xie, J.-S. Lan, X.-B. Wang, N. Jiang, G. Dong, Z.-R. Li, K. D. G. Wang, P.-P. Guo, L.-Y. Kong, Eur. J. Med. Chem. 93 (2015) 42-50. (c) T. Kálai, R. Altman, I. Maezawa, M. Balog, C. Morisseau, J. Petrlova, B. D. Hammock, L.-W. Jin, J. R. Trudell, J. C. Voss, K. Hideg, Eur. J. Med. Chem. 77 (2014) 343-350. (d) S. Thiratmatrakul, C. Yenjai, P. Waiwut, O. Vajragupta, P. Reubroycharoen, M. Tohda, C. Boonyarat, Eur. J. Med. Chem. 75 (2014) 21 -30.

[37] (a) N. P. Selvam, C. Saravanan, D. Muralidharan, P. T. Perumal, *Heterocycl.Chem.* 43 (2006) 1379-1382. (b) N. P. Selvam, P. T. Perumal, Tetrahedron, 64 (2008) 2972-2978.

[38] G. L. Ellman, K. D. Courtney, V. Andres Jr, R. M. Feather-Stone, Biochem. Pharmacol. 7 (1961) 88-90.

[39] G. V. D. Ferrari, M. A. Canales, I. Shin, L. M. Weiner, I. Silman, N. C. Inestrosa, Biochemistry. 40 (2001) 10447-10457.

[40] M. L. Bolognesi, V. Andrisano, M. Bartolini, A. Cavalli, A. Minarini, M. Recanatini, M. Rosini, V. Tumiatti, C. Melchiorre, II Farmaco. 60 (2005) 465-473.

[41] A.K. Sharma, S.T. Pavlova, J. Kim, D. Finkelstein, N.J. Hawco, N.P. Rath, J. Kim, L.M. Mirica, J. Am. Chem. Soc. 134 (2012) 6625-6636.

15 novel tacrine derivatives were synthesized as multifunctional anti-AD agents.

Most of compounds showed excellent inhibition of AChE, BuChE and Aβ aggregation.

Most of compounds showed certain selectivity for AChE over BuChE.

The electron density of phenylacetate is the key to inhibitory activity of AChE.

Compound **7c** was the best compound as out of the synthesized compounds.